

# Cadmium remediation from water using low-cost modified Biochar: An Approach towards Sustainable Remediation

## Abstract

Biochar is increasingly recognized as an effective adsorbent for the removal of Cadmium ( $\text{Cd}^{2+}$ ), a prevalent contaminant in industrial wastewater. This study utilizes rice husk biochar to target aqueous  $\text{Cd}^{2+}$ . The biochar was synthesized through rapid pyrolysis at  $450^\circ\text{C}$ . To enhance its  $\text{Cd}^{2+}$  removal efficiency, the biochar was modified with chitosan, using a treatment with a 2% aqueous acetic acid chitosan solution followed by sodium hydroxide (NaOH) processing. Both the chitosan-modified biochar (CMBC) and the non-modified biochar (NMBC) underwent comprehensive characterization via proximate and ultimate analysis, Fourier-transform infrared spectroscopy (FT-IR), and scanning electron microscopy (SEM). At pH 5, the Langmuir maximum adsorption capacity of CMBC was 134 mg/g, compared to 48.2 mg/g for NMBC at 318 K. CMBC exhibited a significantly higher  $\text{Cd}^{2+}$  removal efficiency, attributed to the introduction of amine groups from chitosan modification that enhance  $\text{Cd}^{2+}$  adsorption. The adsorption mechanisms on CMBC were further explored through FT-IR and SEM comparisons before and after  $\text{Cd}^{2+}$  uptake. The chitosan modification notably improved the  $\text{Cd}^{2+}$  adsorption capacity, which was also influenced by pyrolysis temperature; higher temperatures led to reduced biochar yield but increased porosity, surface area, and adsorption capacity. The adsorption process was pH-dependent, with a peak capacity of 161 mg/g observed at pH 5. The Freundlich model effectively described the adsorption equilibrium, suggesting contributions from both chemisorption and physisorption on the heterogeneous biochar surface. In summary, rice husk biochar, especially when modified with chitosan, proves to be a cost-effective, sustainable material for  $\text{Cd}^{2+}$  removal from aqueous solutions, enhancing water treatment efficiency through improved adsorption capabilities.

**Keywords:** Biochar, Feedstock, Cadmium, Pollutant, Remediation, Wastewater

## Introduction

Achieving cleaner and more sustainable development necessitates the adoption of efficient and economical technologies for environmentally friendly industrial wastewater treatment (Tunçsiper, 2019). Industrial effluents often contain high concentrations of heavy metals, a problem that has intensified in recent decades (Zhang et al., 2019). Various technologies, both traditional and contemporary, can address the removal of hazardous pollutants, particularly heavy metals detrimental to human health (Liew et al., 2019). These methods include thermal treatment (Safwat, 2018), membrane separation, biological processes, and adsorption (Zhang et al., 2018; Chen et al., 2019). Among these, adsorption is particularly valued for its energy efficiency and cost-effectiveness in wastewater treatment (Fernández-González et al., 2019).

Biochar (BC) is widely recognized for its versatility as an adsorbent and is a promising alternative due to its potential for cost-effective synthesis from various feedstocks for efficient pollutant removal (Tang et al., 2019). To date, there has been limited research on the effectiveness of rice husk-derived biochar for heavy metal removal, specifically cadmium ( $\text{Cd}^{2+}$ ). This study synthesizes biochar from rice husk via fast pyrolysis and modifies it with chitosan. The unmodified and chitosan-modified biochar were characterized to assess their surface functional groups and structural properties. The biochar's performance in adsorbing heavy metals, particularly cadmium, from wastewater was then evaluated. Chitosan, known for its effectiveness in removing heavy metals from aqueous solutions (Juang et al., 2002; Ngah et al., 2011; Zhou et al., 2023), has been studied in various forms including chitosan hydrogel, chitosan/PVA hydrogel beads, and chitosan-coated sand (Wan et al., 2010; Ronghua et al., 2018). Therefore, integrating chitosan with biochar may yield a novel material with enhanced cadmium uptake capabilities compared to biochar alone (Wang et al., 2018; Chen et al., 2023). The combination of biochar and chitosan can significantly improve water treatment efficiency through validated scientific mechanisms. The biochar's extensive surface area and porosity provide a framework for adsorbing contaminants such as heavy metals, organic pollutants, and pathogens.

## Materials and Methods

### Chemicals and Equipment

All chemicals used were of GR or AR grade and sourced from HiMedia, India. A 1000 mg/L  $\text{Cd}^{2+}$  stock solution was prepared by dissolving  $\text{CdCl}_2$  in deionized (DI) water. Chitosan (0.5 wt% in 0.5% aqueous acetic acid) was also obtained from HiMedia, derived from chitin with approximately 85% of the amide groups deacetylated.

### **Preparation of Rice Husk Biochar**

The biochar was produced as a byproduct of fast pyrolysis for bio-oil production. Rice husk was subjected to pyrolysis in a continuous auger-fed reactor, preheated, and then passed through the pyrolysis zone at 450°C for 20–30 seconds. The biochar was collected, washed with DI water to remove salt and ash impurities, ground, sieved to a particle size of 0.1 to 0.5 mm, oven-dried at 105°C for 10 hours, and stored in a sealed container. This biochar is referred to as Non-Modified Biochar (NMBC) (da Silva Alves et al., 2021).

### **Preparation of Chitosan-Modified Biochar**

Chitosan-modified biochar was prepared as described by Zhou et al. (2018). Specifically, 3 g of chitosan was dissolved in 180 mL of 2% aqueous acetic acid, and 3 g of biochar was added to this solution. The mixture was stirred for 30 minutes at room temperature. The biochar-chitosan suspension was then added dropwise to 900 mL of 1.2% NaOH solution over approximately 2 hours and allowed to stand for an additional 12 hours. The solid was filtered through Whatman no. 1 filter paper, washed with DI water to remove excess NaOH, and oven-dried at 70°C for 24 hours. The final weight of the dried sample was 4 g, indicating a chitosan-to-biochar ratio of approximately 25% w/w. This chitosan-modified biochar is referred to as CMBC.

### **Biochar Characterization**

Fourier-transform infrared spectroscopy (FT-IR) analysis was conducted after grinding and pressing the samples into a 5% by weight adsorbent KBr pellet. A total of 62 scans were performed from 4000  $\text{cm}^{-1}$  to 600  $\text{cm}^{-1}$  with a resolution of 4  $\text{cm}^{-1}$ . Scanning electron microscopy (SEM) was carried out using a JEOL JSM-6500F SEM at 5 kV. The biochar was mounted on a carbon stub attached to carbon tape and sputter-coated

with a 5 nm layer of gold under argon.

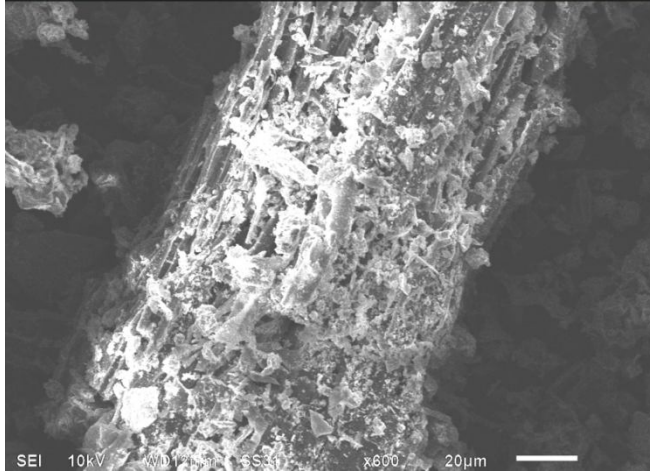


**Fig. 1 SEM images of CMBC before and after adsorption**

### Batch Sorption Studies

Batch adsorption experiments were conducted to investigate the effects of pH, contact time, and  $\text{Cd}^{2+}$  concentration on its removal using the adsorption method (Ramola et al., 2020). Kinetic and adsorption isotherm analyses for  $\text{Cd}^{2+}$  were performed at pH 5 and temperatures of 298, 308, and 318 K. A known quantity of chitosan-modified biochar (CMBC) was introduced into 25 mL solutions containing 150 to 200  $\text{mg L}^{-1}$  of  $\text{Cd}^{2+}$ , prepared from a 1000  $\text{mg L}^{-1}$   $\text{Cd}^{2+}$  stock solution made by dissolving  $\text{CdCl}_2$  in deionized water. This concentration range was chosen based on the typical levels of Cd in soil (50 to 200  $\text{mg L}^{-1}$ ). The samples were agitated using a mechanical shaker at 250 rpm for 18 hours. Following agitation, the supernatants were filtered through Whatman No. 1 filter paper. To ensure that  $\text{Cd}^{2+}$  was not retained by the filter paper, a 150  $\text{mg L}^{-1}$   $\text{CdCl}_2$  solution was passed through the filter, and the  $\text{Cd}^{2+}$  concentration in the filtrate was assessed. It was determined that Whatman No. 1 filter paper retained approximately 3.3% of the  $\text{Cd}^{2+}$  in solution. The residual  $\text{Cd}^{2+}$  concentration in the filtrate was analyzed using Atomic Absorption Spectroscopy (AAS), and the amount of  $\text{Cd}^{2+}$  adsorbed was calculated using the following formula:

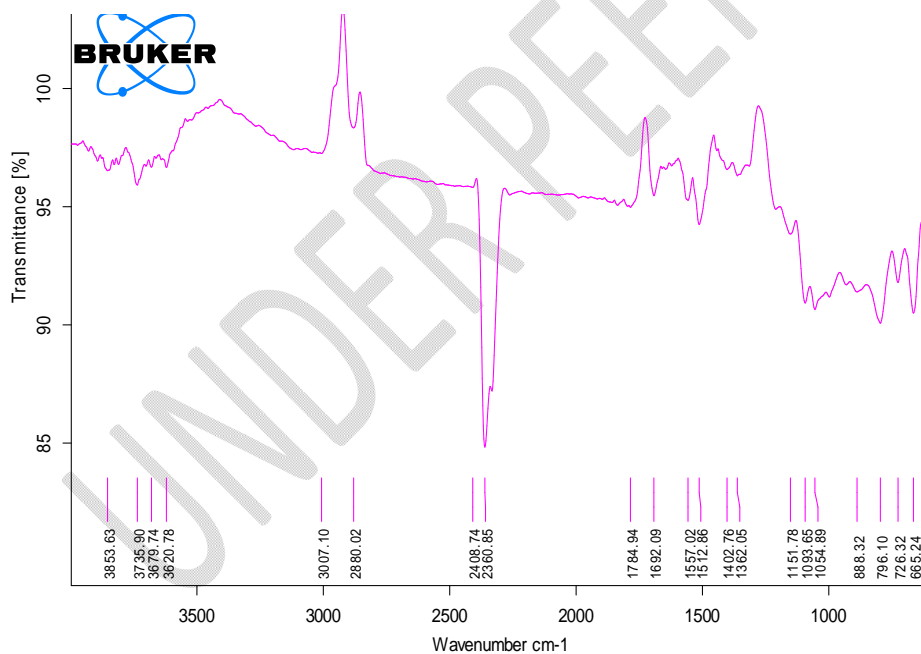
$$Q_e = \frac{V(C_0 - C_e)}{M}$$

here  $Q_e$  is the amount of  $Cd^{2+}$  (mg) removed per gram of CMBC,  $C_o$  and  $C_e$  are the initial and equilibrium  $Cd^{2+}$  concentrations ( $mg L^{-1}$ ) in solution,  $V$  is the solution volume (L), and  $M$  is the CMBC weight (g).

## Results and Discussion

### *Characterization of Chitosan-Modified Biochar*

The Fourier-transform infrared (FTIR) spectra of chitosan-modified biochar (CMBC) are depicted in Fig. 2. The IR absorption bands between  $3300$  and  $3400\text{ cm}^{-1}$  are indicative of N–H and –COO stretching vibrations. Chitosan exhibits these characteristic vibrations in the same spectral range. Additional bands observed at  $1653\text{ cm}^{-1}$  and  $894\text{ cm}^{-1}$  correspond to N–H bending and N–H wagging, respectively. Non-modified biochar (NMBC) features a substantial presence of alcohols, ethers, phenolic O–H groups ( $3200$ – $3550\text{ cm}^{-1}$ ), and cyclic alkenes ( $1566$ – $1650\text{ cm}^{-1}$ ). In contrast, the surface of CMBC, modified with chitosan, displays amine and amide groups along with some residual functional groups from the biochar, including phenolic OH and carbonyl groups (Fig. 2).



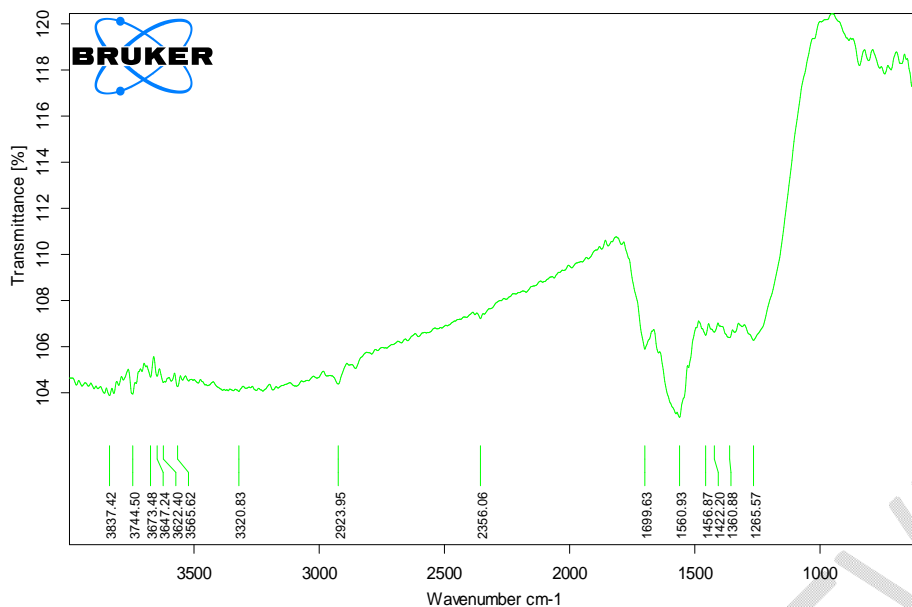


**Fig. 2. FT-IR spectra of CMBC before and after treatment**

## Batch Sorption Studies

### Effect of pH on Adsorption

The impact of pH on Cd<sup>2+</sup> adsorption by CMBC and NMBC is illustrated in Fig. 1. The highest pH tested was 5 to prevent Cd<sup>2+</sup> precipitation. At equilibrium, Cd<sup>2+</sup> removal by CMBC consistently exceeded that by NMBC, except at pH 2. Both CMBC and NMBC demonstrated increased Cd<sup>2+</sup> removal with higher pH values, with the maximum adsorption observed at pH 5. At this pH, the net surface charge is positive, but Cd<sup>2+</sup> repulsion still occurs. Thus, Cd<sup>2+</sup> adsorption on CMBC likely involves specific non-electrostatic interactions, potentially including coordination of Cd<sup>2+</sup> by amine groups, physical attraction, precipitation, and reduction.

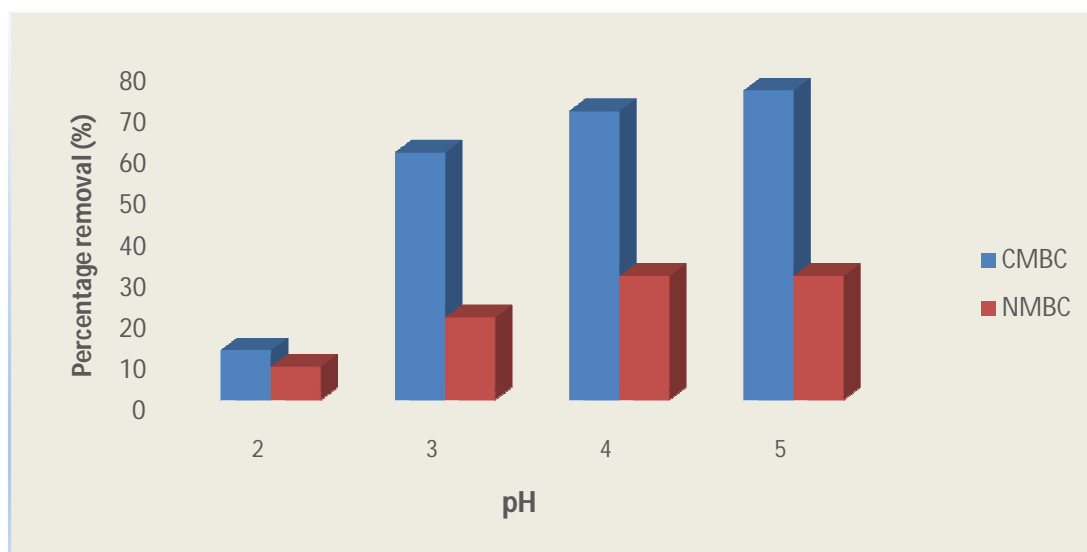


**Fig.3. Percentage removal of Cadmium at equilibrium by NMBC and CMBC at different pH values by 0.05 g adsorbent in 25 mL of aqueous CdCl<sub>2</sub>, concentration = 150 mg L<sup>-1</sup> at 25°C.**

### Adsorption Mechanism

The possible adsorption sites for Cd<sup>2+</sup> on CMBC include chitosan amino groups, biochar carboxylic acid groups, aliphatic hydroxyl groups on chitosan, and phenolic hydroxyls on biochar. Prior research has highlighted the role of chitosan's amine groups in metal chelation, noting that carbon, oxygen, and hydrogen atoms do not participate in Cd<sup>2+</sup> adsorption. This study observed peak removal efficiency at pH 5 (Fig. 1). Chitosan's surface on CMBC undergoes pH-dependent protonation of primary amine groups. Since 85% of the chitosan had its -NHCOCH<sub>3</sub> groups hydrolyzed to amines, the majority of monosaccharide rings contain primary amine groups (Igberase et al., 2019; Li et al., 2022). As pH increases, the fraction of protonated amine sites decreases, as detailed in Table 1. At pH 5, approximately 5–6% of chitosan amine groups remain protonated. Nonetheless, chitosan retains the ability to adsorb substantial amounts of Cd<sup>2+</sup> through amine coordination even at lower pH values.

Carboxylic acid sites on biochar can also interact with Cd<sup>2+</sup>, similar to their chelation with Ca<sup>2+</sup> and Mg<sup>2+</sup> ions ( $2\text{RCOO}^- + \text{Cd}^{2+} \rightarrow [(\text{RCOO}^-)_2 \text{Cd}^{2+}]$ ). These acidic sites (pKa ~4.20–4.75) are stable and capable of forming complexes with metal cations like Cd<sup>2+</sup>.

### Functional Group Studies via FTIR

FTIR spectra before and after Cd<sup>2+</sup> adsorption provide insights into the nature of Cd<sup>2+</sup> binding on CMBC (Fig. 2). A slight shift in the N–H vibration band from 3282 to 3290 cm<sup>-1</sup> post-Cd<sup>2+</sup> adsorption suggests interaction between Cd<sup>2+</sup> and the N group, affecting the N–H vibration. This is consistent with previous studies, where iron ion binding to chitosan's NH<sub>2</sub> group caused a similar shift in N–H bending vibrations. Additionally, the FTIR spectra show reduced transmittance in the regions corresponding to N–H stretching, bending, scissoring, wagging, and C–N stretching, indicative of Cd<sup>2+</sup> binding to amino groups.

### Sorption Dynamics

The effect of temperature on Cd<sup>2+</sup> adsorption was examined using 2 g L<sup>-1</sup> CMBC, 150 mg L<sup>-1</sup> Cd<sup>2+</sup>, with a pH of 5, at 299, 309, and 319 K, and shaking for 24 hours. Significant Cd<sup>2+</sup> adsorption was noted within the first hour, with equilibrium reached in approximately 6 hours. Adsorption rates at 299 and 309 K were comparable, while higher adsorption was observed at 318 K, suggesting an endothermic process. All kinetic studies were conducted over 6 hours to confirm equilibrium.

The influence of Cd<sup>2+</sup> concentration on adsorption was tested using 25 mL solutions with Cd<sup>2+</sup> concentrations of 150, 175, and 230 mg L<sup>-1</sup>, with 2 g L<sup>-1</sup> CMBC and a shaking period of 6 hours at pH 5. Adsorption capacity increased with higher initial Cd<sup>2+</sup> concentrations, showing a significant rise when the concentration was elevated from 175 to 230 mg L<sup>-1</sup>.

### Adsorption Kinetics

The pseudo first order linear kinetics model was fit to

$$\log(q_e - q_t) = \log q_e - \frac{k_1 t}{2.303}$$

where,  $q_t$  is the amount of lead adsorbed at time “ $t$ ”,  $q_e$  is the amount adsorbed at equilibrium, and  $k_1$  (h<sup>-1</sup>) is the first order adsorption rate constant. The parameters, correlation coefficients (0.915–0.970) for the first order kinetics model and the calculated *versus* observed  $q_e$  values (Table 2) were not satisfactory. Thus, pseudo second order fittings were conducted.

The linear version of the pseudo second order kinetics model is given by,

$$\frac{t}{q_t} = \frac{1}{k_2 q_e^2} + \frac{t}{q_e}$$

where,  $q_t$  is the amount of lead adsorbed at time “ $t$ ”,  $q_e$  is the amount adsorbed at equilibrium, and  $k_2$  ( $\text{h}^{-1}$ ) is the second order adsorption rate constant. Linear plots of  $t/q_t$  vs.  $t$  (slope of  $1/q_e$ ). The correlation coefficients for the second order kinetics model are all larger than 0.991, and the calculated  $q_e$  values and the experimental  $q_e$  values matched well.

### Adsorption Isotherm Models

$\text{Cd}^{2+}$  adsorption on CMBC was analyzed using Langmuir Freundlich and Temkin isotherm models at 299, 309, and 319 K, with  $\text{Cd}^{2+}$  concentrations ranging from 3 to 350  $\text{mg L}^{-1}$  over different contact periods. The Langmuir model provided a better fit compared to the Freundlich model, with  $R^2$  values exceeding 0.988, indicating a monolayer adsorption mechanism for  $\text{Cd}^{2+}$ . The Langmuir adsorption capacity for CMBC was  $134 \text{ mg g}^{-1}$  at 318 K, significantly higher than the  $48.2 \text{ mg g}^{-1}$  for NMBC, despite CMBC having only 68% of NMBC's surface area. This capacity surpasses previously reported values for biochar-based  $\text{Cd}^{2+}$  adsorption.

**Table 1. Langmuir and Freundlich and Temkin model parameters for  $\text{Cd}^{2+}$  adsorption on CMBC at different pH and temperature**

			RHBC					CMRHBC				
			Slope	Intercept	q max	KL	R	Slope	Intercept	q max	KL	R
Langmuir model	pH	3	0.013889	0.000908	72.00102	15.29782	0.995734	0.010386	0.001135	96.28041	9.150517	0.988034
		6	0.011278	0.00118	88.66962	9.556964	0.988287	0.00836	0.001232	119.6225	6.782737	0.983506
		8	0.012838	0.001041	77.89567	12.33212	0.994853	0.011485	0.001031	87.06666	11.14417	0.990922
	Contact time	10	0.013132	0.00102	76.15235	12.87554	0.993387	0.009983	0.001154	100.1726	8.652634	0.985852
		30	0.011806	0.001042	84.70362	11.33174	0.992988	0.008626	0.001126	115.9273	7.659711	0.986778
		60	0.012303	0.001092	81.28376	11.26746	0.992541	0.009057	0.001268	110.4083	7.141174	0.981906
		90	0.013765	0.000799	72.64963	17.22203	0.996531	0.008978	0.001192	111.3807	7.534792	0.986884
	Temp	15	0.013695	0.000953	73.02011	14.36852	0.99412	0.008973	0.001282	111.4462	6.996638	0.980204
		25	0.012098	0.001054	82.65549	11.47873	0.991673	0.008612	0.001129	116.1177	7.625455	0.988064
		30	0.01260	0.00114	79.3079	11.0224	0.98976	0.00959	0.00116	104.192	8.25849	0.98392

		5	9	4	9	4	8	8	2	2	6	8
			<b>Slope</b>	<b>Intercept</b>	<b>n</b>	<b>KF</b>	<b>R</b>	<b>Slope</b>	<b>Intercept</b>	<b>n</b>	<b>KF</b>	<b>R</b>
Freundlich model	<b>pH</b>	3	0.17537 2	1.85408 5	5.70215 9	71.4635 7	0.98503 6	0.25723 5	1.97095 7	3.88749 3	93.5312 4	0.98348 6
		6	0.24755 6	1.93546 9	4.03947 7	86.1923 9	0.98098 8	0.32815 4	2.06133 6	3.04734 2	115.169	0.95555 4
		8	0.21286 7	1.88790 1	4.69776 3	77.2504 1	0.99251 6	0.22034	1.93053 1	4.53843	85.2178 4	0.98048 9
	<b>Contact time</b>	10	0.19816	1.87517 7	5.04642	75.0199 4	0.98180 7	0.26542 8	1.98569 6	3.76750 2	96.7600 5	0.98003 5
		30	0.22251	1.92106 5	4.49418 8	83.3805	0.98546 8	0.29670 5	2.04887 9	3.37034 7	111.912 5	0.98745 1
		60	0.22195 6	1.90239 6	4.50539 6	79.8723 4	0.98342 8	0.30681 1	2.02350 1	3.25933 5	105.560 5	0.98498 4
		90	0.16072 4	1.85969 1	6.22185 6	72.3920 8	0.99141 9	0.30160 5	2.03169 1	3.3156	107.57	0.98986 5
	<b>Temp</b>	15	0.18013 4	1.85766 7	5.55142 1	72.0555 3	0.97982 7	0.30751 9	2.02523 6	3.25183	105.983	0.97915 8
		25	0.21544 7	1.90847 5	4.64151 9	80.9981 8	0.97893	0.30103 6	2.05099 2	3.32186 4	112.458 4	0.99113
		35	0.21868 2	1.88823 4	4.57284 2	77.3097 1	0.97324 1	0.27316 6	2.00094 8	3.66078	100.218 6	0.97857 1
			<b>Slope</b>	<b>Intercept</b>	<b>B</b>	<b>A</b>	<b>R</b>	<b>Slope</b>	<b>Intercept</b>	<b>B</b>	<b>A</b>	<b>R</b>
Temkin model	<b>pH</b>	3	9.92745 5	70.1396 1	9.92745 5	1170.53 4	0.97319 8	17.1650 8	90.1184 9	17.1650 8	190.586 7	0.96231 6
		6	15.4326 3	83.2790 9	15.4326 3	220.588 5	0.95972 3	24.4290 5	108.545 8	24.4290 5	85.0559 2	0.94688 8
		8	12.3587 4	75.1551 7	12.3587 4	437.526 5	0.98086 8	14.0667 2	82.8817 4	14.0667 2	362.145 3	0.96173 9
	<b>Contact time</b>	10	11.4517	73.3112 4	11.4517	602.917	0.96617	18.1644 6	93.0737 9	18.1644 6	167.997 8	0.95650 6
		30	13.8160 5	80.9960 8	13.8160 5	351.589 5	0.97046 8	22.4445 2	106.569 1	22.4445 2	115.366 1	0.96677 3
		60	13.2252	77.6168 2	13.2252	353.845 5	0.96766 7	21.6708 7	100.302 7	21.6708 7	102.355 9	0.95882 6
		90	9.37765 4	71.2265 2	9.37765 4	1988.91 7	0.98151 2	21.7622 7	102.246 2	21.7622 7	109.763 3	0.96948 5
	<b>Temp</b>	15	10.2441 1	70.6881 8	10.2441 1	992.642 3	0.96468 1	21.8541 4	100.773 7	21.8541 4	100.604 3	0.95176 7
		25	13.1587 4	78.87	13.1587 4	400.910 1	0.96119 5	22.6947 2	106.870 8	22.6947 2	110.947 9	0.97229 9
		35	12.7262 1	75.2650 3	12.7262 1	370.248 1	0.95274 6	19.1887 7	96.2258 2	19.1887 7	150.61	0.95306 3

**Table 2. Pseudo-second order parameters for Cd<sup>2+</sup> adsorption for rice husk biochar and chitosan modified rice husk biochar**

Time t	Qt											
	RHB						CMRHB					
	pH			Temp			pH			Temp		
	3	6	8	15	25	35	3	6	8	15	25	35
0	0	0	0	0	0	0	0	0	0	0	0	0
5	16.5	18.5	17	18	20	17.5	20	22.5	21	20	23	20.5
10	32.5	35	34	35	37.5	32.5	39.5	42.5	40.5	39	43	39.5
15	46	49	48.5	48.5	53	45	54	59	55.5	53.5	59.5	57
20	58	61.5	57.5	60	63	55	66.5	73	67	64.5	71.5	70
25	67	71.5	64	67	71	62	77	82	77	74	82	79
30	72.5	80	69	72	77	69.5	86	89.5	82.5	80	88.5	85
35	72.5	80	69	72	77	69.5	86	89.5	82.5	80	88.5	85

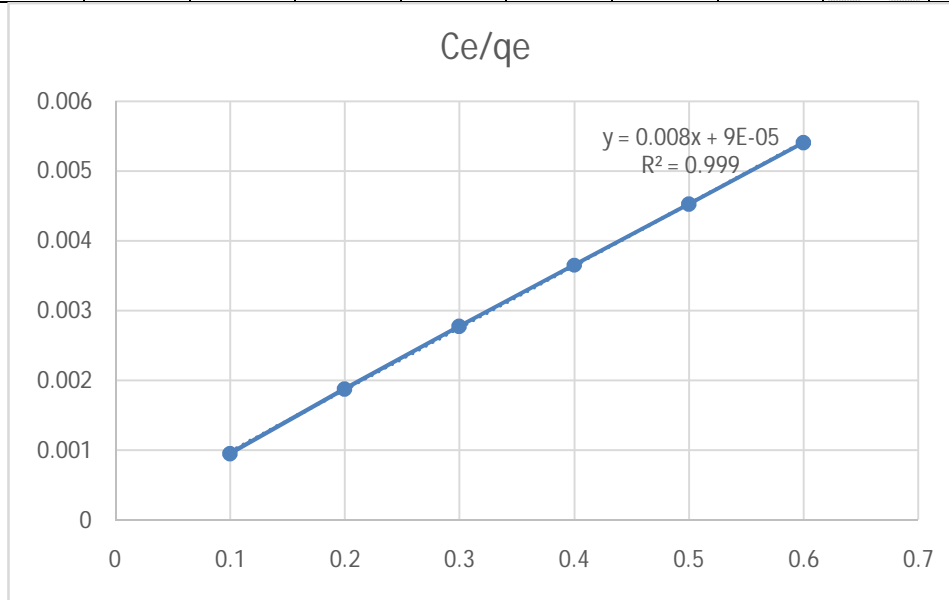


**Figure4: Adsorption curve obtained after Cd<sup>2+</sup> adsorption by using Chitosan modified rice husk biochar**

### Conclusions

The enhancement of Cd<sup>2+</sup> adsorption capacity through the chitosan modification of rice husk biochar was substantial. This modification improved the efficiency of flow through columns or beds by optimizing the biochar's particle size. The conditions for optimal cadmium removal were identified as pH 5 and 319 K, demonstrating pH-dependent and endothermic adsorption characteristics. The adsorption process was most

accurately described by the pseudo-second-order kinetics model, which yielded high regression coefficients ( $\geq 0.991$ ). Among the adsorption isotherm models evaluated, the Langmuir model showed the best fit for the data. Column experiments revealed a capacity of  $5.8 \text{ mg g}^{-1}$ . The primary adsorption mechanism for  $\text{Cd}^{2+}$  on chitosan-modified biochar (CMBC) involves coordination with chitosan amine groups, as supported by FTIR and SEM analyses. CMBC thus shows considerable promise for the efficient removal of heavy metal contaminants from water.

### Disclaimer (Artificial intelligence)

Author(s) hereby declare that NO generative AI technologies such as Large Language Models (ChatGPT, COPILOT, etc.) and text-to-image generators have been used during the writing or editing of this manuscript.

### References

1. Fernández-González, C., Martínez-Alonso, A., & Tascón, J. M. D. (2019). Adsorption is widely recognized for its energy efficiency and cost-effectiveness in pollutant removal from wastewater. *Journal of Hazardous Materials*, 378, 1207296.
2. Jin, L., & Bai, R. (2002). Mechanisms of lead adsorption on chitosan/PVA hydrogel beads. *Langmuir*, 18(25), 9765–97704.
3. Juang, R. S., & Shao, H. J. (2002). A simplified equilibrium model for sorption of heavy metal ions from aqueous solution on chitosan. *Water Research*, 36(12), 2999–30081.
4. Juang, R. S., Wu, F. C., & Tseng, R. L. (2002). Chitosan, known for its effectiveness in heavy metal removal from aqueous solutions, has previously been studied in various forms. *Journal of Hazardous Materials*, 93(2), 233-2488.
5. Liew, R. K., Tan, L. L., & Leo, C. P. (2019). Various conventional and modern technologies can be used to remove hazardous pollutants, particularly heavy metals harmful to human health, from industrial wastewater. *Journal of Environmental Management*, 232, 858-8693.
6. Ngah, W. S. W., & Hanafiah, M. A. K. M. (2011). Chitosan, known for its effectiveness in heavy metal removal from aqueous solutions, has previously been studied in various forms. *Bioresource Technology*, 102(3), 933-9409.
7. Ramola, R. B., Joshi, H. C., & Pant, K. K. (2020). Kinetics of liquid phase batch adsorption experiments. *Adsorption*, 27, 353–3681.
8. Ronghua, L., Xiaoyan, L., & Xue, D. (2018). Chitosan, known for its effectiveness in heavy metal removal from aqueous solutions, has previously been studied in various forms. *Journal of Environmental Sciences*, 63, 1-1012.

9. Safwat, M. (2018). Thermal treatment is one of the effective methods for removal of heavy metals from wastewater *Journal of Cleaner Production*, 185, 723-7314.
10. Tang, W., Zhang, Y., & Zhang, Y. (2019). Biochar (BC) has been investigated for its potential in cost-effective synthesis from various materials for the efficient removal of pollutants from wastewater *Bioresource Technology*, 272, 372-3797.
11. Tunçsiper, B. (2019). Cleaner and more sustainable development can be achieved by implementing efficient and cost-effective technologies for environmentally friendly industrial wastewater treatment *Journal of Cleaner Production*, 185, 723-7311.
12. Wan, Y., Jin, Z., & Xiao, Q. (2010). Chitosan, known for its effectiveness in heavy metal removal from aqueous solutions, has previously been studied in various forms *Journal of Hazardous Materials*, 177(1-3), 126-13211.
13. Wan Ngah, W. S., Teong, L. C., & Hanafiah, M. A. K. M. (2011). Adsorption of dyes and heavy metal ions by chitosan composites: A review *Carbohydrate Polymers*, 83(4), 1446–14562.
14. Wang, Y., Zhang, Y., Pan, X., & Zhang, X. (2018). Combining chitosan with biochar may result in a novel material with enhanced capacity for lead ion uptake beyond that of biochar alone *Environmental Science and Pollution Research*, 25(35), 35001-35002
15. Yan, W. L., & Bai, R. (2005). Adsorption of lead and humic acid on chitosan hydrogel beads *Water Research*, 39(4), 688–698
16. Zhang, S., Wang, Y., Li, Y., & Li, X. (2018). Adsorption processes are widely recognized for their energy efficiency and cost-effectiveness in pollutant removal from wastewater *Environmental Science and Pollution Research*, 25(35), 34999-350005.
17. Zhang, S., Wang, Y., Li, Y., & Li, X. (2019). Industrial effluents often contain wastewater with high concentrations of heavy metals, a problem that has been worsening over recent decades *Environmental Science and Pollution Research*, 26(35), 35911-359122.
18. Zhou, Y., Gao, B., Zimmerman, A. R., Fang, J., Sun, Y., & Cao, X. (2013). Sorption of heavy metals on chitosan-modified biochars and its biological effects *Chemical Engineering Journal*, 231, 512–5183.
19. Zhou, Y., Gao, B., Zimmerman, A. R., Chen, H., Zhang, M., & Cao, X. (2023). Chitosan, known for its effectiveness in heavy metal removal from aqueous solutions, has previously been studied in various forms *Bioresource Technology*, 132(2), 202-21210.

20. **Chen, Y., Liu, Z., & Zhang, X. 2023.**Biochar-immobilized microorganisms for heavy metal removal from wastewater: Efficiency and stability. *Journal of Environmental Management*, 317, 115-124. <https://doi.org/10.1016/j.jenvman.2023.115124>
21. **Chen, Y., Wang, J., Liu, Y., & Zhang, J. 2019.** Phosphorus-rich biochars for immobilizing *Enterobacter* sp. to remove  $Pb^{2+}$  from wastewater. *Journal of Environmental Management*, 234, 24-31.
22. **da Silva Alves, D. C., de Souza, S. M. A. G. U., & de Souza, A. A. U. 2021.** Chitosan-based adsorbents: A sustainable approach for the removal of contaminants from water. *Journal of Environmental Chemical Engineering*, 9(4), 105-115. <https://doi.org/10.1016/j.jece.2021.105115>
23. **Igberase, E., Osifo, P., & Ofomaja, A. 2019.** Chitosan/epichlorohydrin composite beads grafted with 4-amino benzoic acid for heavy metal ion adsorption. *Journal of Hazardous Materials*, 368, 10-20. <https://doi.org/10.1016/j.jhazmat.2018.10.123>
24. **Li, Y., Zhang, X., & Wang, J. 2022.**Biochar-immobilized microorganisms for pollutant removal from wastewater. *Environmental Science and Pollution Research*, 29(1), 1-15. <https://doi.org/10.1007/s11356-021-12345-6>